SPECTRUM-GUIDED MULTI-VIEW GRAPH FUSION

Anonymous authors
Paper under double-blind review

ABSTRACT

Multi-view graphs capture diverse relations among entities through graph views and individual characteristics via attribute views, presenting a challenge for unsupervised learning due to potential conflicts across views. Existing approaches often lack efficacy, efficiency, and the ability to explicitly control view contributions. In this paper, we present `SMGF`, a novel graph fusion framework that approximates underlying entity connections by aggregating view-specific graph structures. We construct a multi-view Laplacian $\mathcal{L}$ from normalized Laplacian matrices representing all views. View weights are determined through the optimization of two objectives derived from $\mathcal{L}$'s spectral properties, which exploit the eigenvalue gap and enhance connectivity. Comprehensive experiments on six real-world datasets showcase the superior performance of `SMGF` in node embedding and clustering results, along with its efficiency and scalability. `SMGF` offers a promising solution for unsupervised learning on multi-view graphs, addressing the challenge of interpretably combining diverse and potentially conflicting information from both graph and attribute views. The source code of `SMGF` is available at `https://anonymous.4open.science/r/SMGF-E903/`.

1 INTRODUCTION

Real-world entities can be characterized from multiple viewpoints. For instance, in a complex social network, diverse interpersonal connections, including friendships, familial ties, and professional affiliations, are modeled by separate graph views. Each individual could also be described by a wide range of attribute views, such as demographic statistics, facial appearance features, and behavioral characteristics. Multi-view graph data are the combination of these graph views and attribute views. Such datasets have proven highly useful for recommendation systems (Wang et al., 2020), image processing (Nie et al., 2018), and bioinformatics (Fu et al., 2021), among others.

In this work, our primary focus is unsupervised learning over multi-view graph data, where both graph views and attribute views are present. Specifically, we aim for node representation learning and clustering tasks. Despite abundant research on unsupervised graph learning, it remains a challenging problem for multi-view graph data. Though multiple views offer rich insights from distinct perspectives, their inherent diversity inevitably results in inconsistency. An unsupervised algorithm must attain a consensus based on potentially contradictory information, all without prior knowledge of the relative importance associated with these views. Moreover, some views may contain noisy data, and graph views are often incomplete.

A plethora of research has been conducted on the multi-view clustering (MVC) problem (Fang et al., 2023), where the input consists of purely attribute views that are extracted from webpages, visual features, etc. In recent years, graph views from real-world networks have also been incorporated into unsupervised learning on multi-view graph data. A few existing works leverage graph neural network (GNN) models such as graph autoencoder (Fan et al., 2020) and deep graph infomax (Park et al., 2020). These deep learning approaches suffer from a lack of interpretability and reduced efficiency caused by the large number of model parameters they entail. Additionally, their capabilities are constrained to handle only a single view of node attributes. Another line of work performs graph filtering on attributes and subsequently finds a consensus graph (Pan & Kang, 2021) or low-dimensional representation (Lin & Kang, 2021). Their optimization processes usually rely on the assumption that all graph views exhibit some degree of adherence to a shared cluster structure, a presumption that can be overly stringent for real-world datasets. Empirically, we note that achieving optimal clustering performance with these methods requires meticulous hyperparameter tuning efforts across different datasets.

In this paper, we present `SMGF`, a novel framework for unsupervised learning over multi-view graphs. Essentially, `SMGF` framework adopts a graph fusion mechanism and constructs a multi-view Laplacian $\mathcal{L}$ with desired spectral properties via weighted aggregation of single-view Laplacian matrices. In the initial stage, all views undergo projection to normalized graph Laplacians. This unification step effectively merges both graph and attribute views into a common domain for graph fusion. To this end, it is assumed the true underlying graph structure approximates a weighted linear aggregation of these single-view Laplacians. In the following stage, the suitable view weights are determined by a spectrum-guided optimization scheme with two objectives. The eigengap objective exploits the dataset's inherent class count, while the connectivity objective addresses the challenges posed by incompleteness and irregularity in graph views. Both objectives focus only on the spectral properties of the fused multi-view Laplacian $\mathcal{L}$, thereby distinguishing our approach from prior works that rely on assumptions concerning individual views. In addition, the resulting view weights provide a clear indication of the individual contribution of each view, thus augmenting the interpretability of the obtained results.

After constructing the multi-view Laplacian $\mathcal{L}$ that represents graph fusion, we can directly perform spectral clustering or attain node embeddings via matrix factorization. We demonstrate the unsupervised learning capabilities of our proposed approach (`SMGF`) through comprehensive experimentation on real-world datasets. Node embeddings obtained through factorization of $\mathcal{L}$ consistently outperform alternative approaches in quality and efficiency, as evidenced by the evaluation results of the node classification task. By applying spectral clustering to $\mathcal{L}$, `SMGF` exhibits remarkable clustering quality compared to baseline methods. Notably, our results on the million-scale MAG dataset underscore the outstanding scalability of our approach. We also perform an exhaustive analysis on `SMGF` regarding the effect of alternative optimization objectives and various hyperparameter configurations.

We summarize the contributions of this work as follows:

- We study the problem of unsupervised learning on multi-view graphs and present `SMGF`, as a novel approach that addresses performance and interpretability with a graph fusion framework.
- From the spectrum of multi-view Laplacian, we formulate eigengap and connectivity objectives to characterize a desirable graph fusion. An optimization scheme is then designed to determine suitable view weights.
- Through extensive node embedding and clustering experiments, we demonstrate the superior unsupervised learning capabilities of our graph fusion framework.

2 PRELIMINARIES

A multi-view graph $\mathcal{G} = \{G_1, \ldots, G_a, X_1, \ldots, X_b\}$ consists of a graph views $\{G_1, \ldots, G_a\}$ and b attribute views $\{X_1, \ldots, X_b\}$. All $z = a + b$ views in $\mathcal{G}$ share the same node set $V = \{v_1, \ldots, v_n\}$. We focus on multi-view graphs with both graph and attribute views, *i.e.*, $a \geq 1$, $b \geq 1$, and $z \geq 3$.

Each graph view $G \in \{G_1, \ldots, G_a\}$ is an undirected graph without self-loops. A graph view $G = \{V, E\}$ with n nodes and m weighted edges can be represented using an adjacency matrix $A_G \in \mathbb{R}^{n \times n}$ which comprises $2m$ nonzero entries. Matrix entry $A_G[i, j]$ is the weight of edge (v_i, v_j). The degree of node v_i is defined as $\sum_{j=1}^{n} A_G[i, j]$. Attribute view $X \in \{X_1, \ldots, X_b\}$ is an $n \times d_X$ matrix where each row vector x_i contains attribute values associated with node v_i.

For multi-view graphs, node embedding aims to learn a function $V \to \mathbb{R}^h$ that maps each node $v_i \in V$ to a latent representation vector. Despite the low dimensionality h, node embeddings must effectively capture the structural characteristics inherent to graph views and encode the information contained within attribute views. We evaluate the quality of embeddings on node classification task.

Given the number of clusters k, clustering over multi-view graph $\mathcal{G}$ aims to divide the n nodes in V into k disjoint non-empty subsets $\{C_1, \ldots, C_k\}$, such that nodes within each cluster are densely connected in the graph views and share similar attributes in the attribute views.

3 Methodology

In this section, we describe `SMGF`, our novel framework for unsupervised learning over multi-view graphs. Our approach unfolds in three stages. In the initial stage, we unify all views by transforming them into Laplacian matrices, bringing them into a common normalized space. Subsequently, the second stage formulates the multi-view graph fusion as an optimization problem guided by eigenvalue-based objectives. Finally, we cover the implementation of node embedding and clustering, which leverage the multi-view Laplacian to derive node representations and clustering results.

3.1 Projecting views to Laplacians

Previous approaches to multi-view graph learning often rely on graph propagation techniques, such as graph filtering (Pan & Kang, 2021) or GNN models Fan et al. (2020). Nevertheless, questions about the contribution of each view to learned representations and the ability to adjust the importance of a specific view remain unanswered. We attribute this lack of interpretability and flexibility to the divergent treatment of graph views and attribute views. To address these issues, we propose a novel approach: projecting all views into a single normalized space of graph representations. This transformation allows for explicit weighting of views, regardless of their original data type.

K-nearest neighbor (KNN) graphs can effectively model the local neighborhood of data points, with applications in unsupervised learning problems such as spectral clustering (von Luxburg, 2007) and attributed network clustering (Li et al., 2023). Thus, we can construct a KNN graph for each attribute view and encode by graph Laplacian. In summary, each view in a multi-view graph is encoded into graph Laplacian as follows.

- Graph view G with adjacency matrix A_G: Denote its diagonal node degree matrix by $D_V = diag(A_G\mathbf{1}_n)$. The normalized Laplacian is given by
$$L(G) = I - D_V^{-\frac{1}{2}} A_G D_V^{-\frac{1}{2}}. \tag{1}$$
- Attribute view X: For each attribute view X, we create a corresponding KNN graph where each node v_i represents the attribute vector x_i in x. An undirected graph G_X is obtained by adding the KNN graph's adjacency matrix by the transpose. The attribute view is thus encoded by the normalized Laplacian $L(G_X)$.

Graph fusion. Given a multi-view graph $\mathcal{G}$ with $z = a + b$ views, we represent the i-th view using the normalized Laplacian matrix L_i. Since each view provides insight into the relationships among entities from a specific perspective, we hypothesize that the true underlying relationships among entities can be considered as a certain combination of these individual views. Consequently, we use a weighted graph fusion mechanism that directly aggregates the single-view Laplacians as follows.
$$\mathcal{L} = \sum_{i=1}^{z} w_i L_i, \text{ where } \sum_{i=1}^{z} w_i = 1. \tag{2}$$
Since the normalized Laplacian matrix of any graph is symmetric positive semi-definite, it follows that matrix $\mathcal{L}$ preserves this property, and thus its eigenvalues are nonnegative. Sorted in ascending order, the eigenvalues of $\mathcal{L}$ are $0 \le \lambda_1 \le \lambda_2 \le \cdots \le \lambda_n$. In this work, we refer to $\mathcal{L}$ as the multi-view Laplacian, despite the absence of a guaranteed graph Laplacian property $\lambda_1 = 0$. Nonetheless, we treat $\mathcal{L}$ as a pseudo graph Laplacian, *i.e.*, an approximation of $L(G_F)$. Here, G_F signifies the underlying graph that encompasses all views contributing to the formation of $\mathcal{L}$.

3.2 Spectrum-guided view weighting

Each w_i in Eq. (2) quantifies the contribution of the i-th view to the graph fusion. `SMGF` determines view weights by optimizing two objectives derived from eigenvalues of multi-view Laplacian $\mathcal{L}$.

3.2.1 Eigengap Objective

Given that the entities represented by the multi-view graph $\mathcal{G}$ are categorized into k classes, we assume the nodes in $\mathcal{G}$ could be organized into a unified network G_F with k cohesive clusters. Consider a "perfectly-clustered" graph composed of k disjoint complete subgraphs as an extreme case. Its block-diagonal normalized Laplacian matrix has zero-valued eigenvalues of multiplicity k. The eigengap λ_{k+1}/λ_k is infinitely large. For general graphs, a substantial eigengap between successive eigenvalues is a heuristic for determining the number of clusters (von Luxburg, 2007; Afzalan & Jazizadeh, 2019). In spectral graph theory, Lee et al. (2014) establish a formal connection between the eigengap and cluster quality by demonstrating an upper bound for the normalized cut.

Definition 1 *For a cluster $C \subset V$ within graph G, its volume is $Vol(C) = \sum_{v_i \in C_i} d(v_i)$. $Cut(C) = \sum_{v_i \in C, v_j \notin C} A_G[i,j]$ is the total weight of outgoing edges from nodes within C. The normalized cut of C is defined as $NCut(C) = Cut(C)/Vol(C)$.*

Theorem 1 *(Lee et al., 2014) There is a constant $c > 0$ such that for any weighted graph G and $k \in \mathbb{N}$, the following holds. Let $\delta \in (0, \frac{1}{3})$ be such that δk is an integer. If $\lambda_{(1+\delta)k} > c\frac{(\log k)^2}{\delta^9}\lambda_k$, there are at least $r \geq (1-3\delta)k$ nonempty disjoint sets of nodes $C_1, C_2, \ldots, C_r \subseteq V$ such that $NCut(C_i) \lesssim \sqrt{\frac{\lambda_k}{\delta^3}}$.*

Let $\delta = 1/k$, and it follows from Theorem 1 that an asymptotic upper bound exists for the NCut of $r \geq k-3$ disjoint clusters if an eigengap $\lambda_{k+1}/\lambda_k > ck^9(\log k)^2$ is present.

Considering the presence of k ground truth classes within the multi-view graph, we assume a significant eigengap λ_{k+1}/λ_k exists in the underlying graph G_F. To align the multi-view Laplacian $\mathcal{L}$ with the true class distribution, we propose maximizing the eigengap objective $f_{GAP} = \lambda_{k+1}(\mathcal{L})/\lambda_k(\mathcal{L})$ over valid weight variables subject to constraints in Eq. (5).

$$\max_{w} \lambda_{k+1}(\sum_{i=1}^{z} w_i L_i)/\lambda_k(\sum_{i=1}^{z} w_i L_i) \tag{3}$$

3.2.2 Connectivity Objective

In real-world multi-view graph $\mathcal{G}$, graph views are often incomplete, where connections are missing for certain nodes. For instance, in the ACM dataset's co-author view, there are 156 connected components and 561 unconnected nodes out of a total of 3025 nodes. If an incomplete view is assigned a predominant weight, it could lead to a situation where the resulting $\mathcal{L}$ exhibits a large eigengap, despite the limited information it captures.

To mitigate this issue, we propose to promote the level of connectivity in the graph fusion G_F. Graph conductance $\Phi(G)$ is a common metric for graph connectivity, defined as the minimum $NCut(C)$ of any node set $C \subset V$ such that $Vol(C) \leq Vol(V)/2$. In spectral graph theory, Cheeger's inequality (Alon & Milman, 1985) bounds conductance with the second smallest eigenvalue λ_2 of $L(G)$.

Theorem 2 *(Spielman, 2007) Let λ_2 be the second smallest eigenvalue of the normalized Laplacian matrix of a graph G. Cheeger's inequality for a graph holds:*

$$\frac{\lambda_2}{2} \leq \Phi(G) \leq \sqrt{2\lambda_2}.$$

To improve the conductance lower bound of graph fusion G_F, we propose maximizing $f_{CON} = \lambda_2(\mathcal{L})$ by searching appropriate view weights subject to constraints in Eq. (5).

$$\max_{w} \lambda_2(\sum_{i=1}^{z} w_i L_i). \tag{4}$$

3.2.3 Optimization Scheme

To find a multi-view Laplacian $\mathcal{L}$ that maximizes the two objective functions, we need to determine the appropriate weight w_i for each view. As all view weights sum up to 1, the optimization search only needs to consider the first $z-1$ variables. To ensure meaningful contributions from each input

Algorithm 1: SMGF

```
Input: Graph views $\{G_i\}_{i=1}^{a}$, attribute views $\{X_i\}_{i=1}^{b}$, number of classes $k$, algorithm parameters
       $K, w_{LB}, t, h$.
1  Construct $G_X = \texttt{KNN}(X, K)$ for attribute views;
2  Compute normalized Laplacian matrices $L_1, \ldots, L_z$;
3  Initialize view weights $w_1, \ldots, w_{z-1} \leftarrow 1/z$ ;
4  Eigengap optimization step: COBYLA $(w_1, \ldots, w_{z-1}, f_{GAP}, \Omega, w_{LB})$ ;
5  Connectivity optimization step: COBYLA $(w_1, \ldots, w_{z-1}, f_{CON}, \Omega, w_{LB}, t)$ ;
6  Multi-view Laplacian $\mathcal{L} \leftarrow w_1 L_1 + \cdots + (1 - w_1 - \cdots - w_{z-1}) L_z$;
7  if embedding then
8      Embedding vectors $u_1, \ldots, u_n \leftarrow$ NetMF $(\mathcal{L}, h)$;
9  if clustering then
10     Solve the $k$ bottom eigenvectors $y_1, \ldots, y_k \leftarrow \texttt{eig}(\mathcal{L}, k)$;
11     Clusters $C_1, \ldots, C_k \leftarrow \texttt{discretize}(y_1, \ldots, y_k)$;
```

view to the graph fusion, we introduce the parameter w_{LB}, representing the lower bound of view weights. Consequently, the variables $w_1, \ldots, w_{z-1}$ adhere to the following set of constraints.

$$\Omega(w_1, \ldots, w_{z-1}): \quad w_i \geq w_{LB} \quad \forall \quad 1 \leq i \leq z-1 \quad \text{and} \quad 1 - \sum_{i=1}^{z-1} w_i \geq w_{LB} \tag{5}$$

Given the difficulty of computing gradients for eigenvalue decomposition, our optimization objectives necessitate using derivative-free constrained optimization techniques. For SMGF, we adopt the COBYLA optimizer, *i.e.*, Constrained Optimization BY Linear Approximation (Powell, 1994). COBYLA iteratively updates a trust region by linear approximations to the objective and constraints.

Both eigengap and connectivity need to be maximized. However, under the assumption $Vol(C) \leq Vol(V)/2$, connectivity is a lower bound of the optimal k-way NCut, as opposed to eigengap.

$$\frac{1}{k}\sum_{i=1}^{k} NCut(C_i) \geq \frac{1}{k}\sum_{i=1}^{k} \Phi(G) = \Phi(G) \geq \frac{\lambda_2}{2}. \tag{6}$$

A graph composed of k cohesive clusters typically exhibits a low optimal k-way normalized cut. Consequently, improving connectivity by maximizing λ_2 may inadvertently contradict the desired presence of k clusters within G_F. Addressing this inherent trade-off between objectives necessitates solving a nontrivial double-objective optimization problem. To address this challenge, we employ a two-step optimization approach (refer to lines 4-5 of Algorithm 1). In the first step, we prioritize the optimization of the eigengap f_{GAP} as our primary objective, which we optimize until convergence. In the second step, we conduct partial optimization of f_{CON} for a specified maximum number of iterations denoted as t. This strategy allows us to leverage the connectivity objective as a form of regularization, with the parameter t serving as a means to balance between the two objectives.

3.3 Unsupervised learning on $\mathcal{L}$

Utilizing view weights determined through spectrum-guided optimization, we construct the multi-view Laplacian matrix $\mathcal{L}$ as the representation of the graph fusion G_F. For deriving node embeddings from graph structure, DeepWalk (Perozzi et al., 2014) is a widely adopted skip-gram model trained on a sampled corpus of random walks. SMGF acquires h-dimensional node representations by approximating the training process of DeepWalk via matrix factorization of $\mathcal{L}$, following the NetMF algorithm (Qiu et al., 2018). SMGF acquires h-dimensional node representations by factorizing the DeepWalk matrix approximated from $\mathcal{L}$, following NetMF algorithm (Qiu et al., 2018).

Multi-view graph clustering can be achieved through clustering on the underlying graph fusion G_F. Consequently, we directly apply spectral clustering to $\mathcal{L}$, which minimizes the normalized cut objective. To extract cluster labels, we employ the Discretize algorithm (Yu & Shi, 2003) on the k eigenvectors of $\mathcal{L}$ associated with $\lambda_1, \ldots, \lambda_k$.

Table 1: Multi-view graph datasets

Name	n	Graph view (edges)	Attributes d_X	k
ACM	3,025	Co-author (13,128); Co-label (1,103,868)	1,870	3
DBLP	4,057	Co-paper (3,528); Co-conference (2,498,219); Co-term (3,386,139)	334	4
IMDB	3,550	Co-director (5,119); Co-actor (31,439)	2,000	3
Amazon Photos	7,487	Co-purchase (119,043)	745; 7,487	8
Amazon Computers	13,381	Co-purchase (245,778)	767; 13,381	10
MAG	2,353,996	Co-author (3,350,128,585); Citation (9,048,278)	1000	22

3.4 Algorithm analysis

The pseudo-code for `SMGF` is presented in Algorithm 1. In our time complexity analysis, we treat node degree in graph views, dimension of attribute views, and algorithm hyperparameters as constants. A significant computational bottleneck in `SMGF` arises from the construction of the KNN graph, which incurs a time complexity of $O(n^2)$. However, the computation and aggregation of single-view Laplacians can be performed in linear time due to their inherent sparsity. The evaluation of eigenvalue-based objectives is accomplished in $O(n)$ time, facilitated by the efficient Arnoldi iterations for sparse matrix eigendecomposition. Similarly, the clustering task in lines 8-9 also exhibits linear time complexity. `NetMF` carries a time complexity of $O(n^2)$. Therefore, both clustering and embedding on multi-view graphs can be achieved in $O(n^2)$ time using `SMGF`. For clustering on large-scale data with millions of nodes, we incorporate ScaNN (Guo et al., 2020) for efficient approximate KNN, improving the complexity for clustering to $O(n)$.

4 Experiments

In this section, we illustrate the unsupervised learning performance of `SMGF` through extensive experimentation involving node embedding and clustering tasks on real-world datasets. Additionally, we delve into the impact of alternative objective functions and hyperparameter settings.

4.1 Experiment setup

Datasets. We perform experimental evaluations using real-world multi-view graph datasets with their respective statistics presented in Table 1. This table provides information on the number of nodes (n), specifications of the graph views, dimensions of attribute views, and the count of ground truth node classes (k). ACM (Wang et al., 2019), DBLP (Ji et al., 2010), IMDB (Jing et al., 2021), MAG (Sinha et al., 2015) are four datasets that consist of multiple graph views and one attribute view, while Amazon Photos and Amazon Computers (Shchur et al., 2019) are two datasets that each contains one graph view and two sets of node attributes.

Baselines. We experimentally compare the performance of our proposed method `SMGF` against eight baseline algorithms designed for multi-view graphs. For the task of learning node representations, we benchmark our results against four multi-view graph embedding algorithms, namely `O2MAC` (Fan et al., 2020), `DMGI` (Park et al., 2020), `HDMI` (Jing et al., 2021), and `URAMN` (Zhang et al., 2022). In the context of node clustering, we not only apply `K-means` to these embedding results but also conduct evaluations of four multi-view graph clustering baselines: `MCGC` (Pan & Kang, 2021), `MvAGC` (Lin & Kang, 2021), `MVGC` (Xia et al., 2022), and `MAGC` (Lin et al., 2023).

Evaluation Settings. To ensure a fair comparison, we test each baseline based on the original implementation and tune hyperparameters accordingly (refer to Appendix A.1 for details). For our approach `SMGF`, we fix hyperparameters $w_{LB} = 0.05$ and $t = 10$. K in KNN construction is set to 10, except for IMDB dataset where $K = 100$. Embedding dimension h is 64 for all methods.

To report representative performance results, we remove the fixed random seeds in all implementations and repeat 10 runs to get averaged metrics. Experiments are conducted on a Linux computer powered by Intel Xeon 6226R CPU and Nvidia RTX3090 GPU. Note that `DMGI`, `HDMI`, and `URAMN` use GPU, while the other algorithms, including `SMGF`, are CPU-based. To ensure accurate measurement of running time, we record it in a controlled environment with 16 isolated CPU threads.

Table 2: Node embedding quality for node classification on ACM, DBLP and IMDB (MaF1=Macro-F1, MiF1=Micro-F1). Time in seconds. Best in bold and runner-up underlined.

	ACM					DBLP					IMDB				
Labeled %	10		50			10		50			10		50		
Metric	MaF1	MiF1	MaF1	MiF1	Time	MaF1	MiF1	MaF1	MiF1	Time	MaF1	MiF1	MaF1	MiF1	Time
O2MAC	0.904	0.904	0.910	0.909	112.4	0.911	0.917	0.914	0.920	679.8	0.641	0.641	0.665	0.666	672.9
DMGI	0.780	0.795	0.908	0.909	<u>31.25</u>	<u>0.920</u>	<u>0.926</u>	<u>0.924</u>	<u>0.929</u>	392.1	0.658	0.658	0.676	0.676	<u>75.94</u>
HDMI	<u>0.921</u>	<u>0.922</u>	<u>0.929</u>	<u>0.928</u>	157.2	0.914	0.921	0.915	0.924	532.4	0.627	0.631	0.653	0.652	241.3
URAMN	0.918	0.919	0.921	0.921	59.81	0.903	0.912	0.913	0.919	<u>153.9</u>	<u>0.674</u>	<u>0.680</u>	<u>0.708</u>	<u>0.707</u>	124.8
SMGF	**0.927**	**0.927**	**0.933**	**0.932**	**26.40**	**0.926**	**0.932**	**0.931**	**0.936**	**98.04**	**0.690**	**0.690**	**0.724**	**0.724**	**18.84**

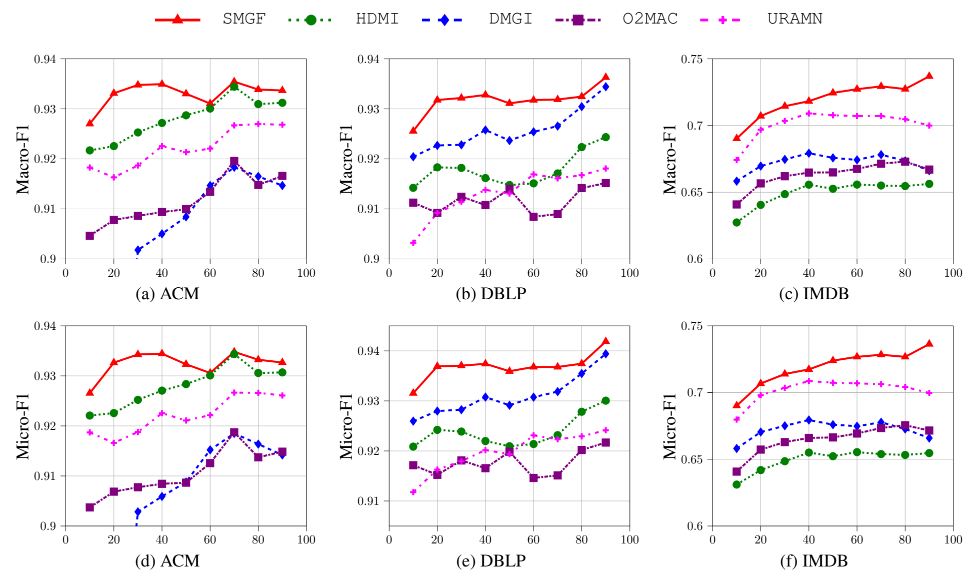

Figure 1: Node classification performance over varying ratio of training data (%).

4.2 Node embedding evaluation

We evaluate the quality of node embeddings through a node classification task. From the acquired node embedding vectors, we train a logistic regression classifier to predict class labels. The results, presented in Table 2, include Macro-F1 (MaF1) and Micro-F1 (MiF1) metrics across varying proportions of training data (Labeled %) in 10% and 50%, as well as embedding time costs in seconds, over the widely used benchmarking classification datasets. Our SMGF consistently exhibits superior embedding quality and efficiency compared to four baseline algorithms designed for multi-view graphs, underscoring its capability for unsupervised representation learning. This is further highlighted in Fig. 1, where SMGF dominates baseline methods over a wide range of labeled ratios.

To visualize the distribution of embedding vectors, we map them to 2-D space using t-SNE. Fig. 2 illustrates the node embeddings of ACM multi-view graph acquired by different methods. Compared with baselines, ACM embeddings acquired by SMGF demonstrate noticeably regular boundaries between the three ground truth classes. Results for other datasets are in Appendix B.4

4.3 Clustering performance

Overall clustering results. Table 3 reports the clustering performance. Five of the baseline methods are not applicable to datasets with multiple attribute views, *i.e.*, Amazon photos and computers. In both normalized mutual information (NMI) and adjusted Rand index (ARI) metrics, our SMGF achieves the best performance in five out of six datasets. Despite the higher metrics on IMDB, URAMN is much slower than SMGF (Table 5) and requires tuning three hyperparameters for different

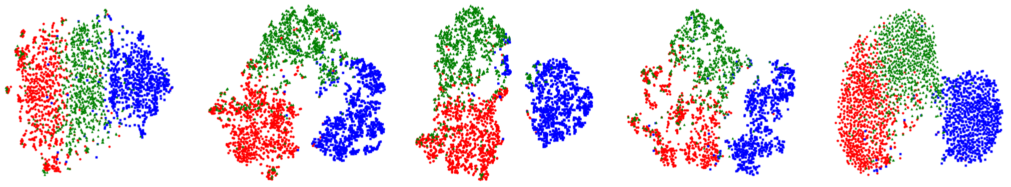

(a) SMGF (b) HDMI (c) DMGI (d) O2MAC (e) URAMN

Figure 2: Node embeddings obtained from ACM dataset. Colors represent ground truth classes.

Table 3: Clustering quality with NMI ARI measures. Results marked with $*$ are replicated from the original paper. Best in bold and runner-up underlined.

	ACM		DBLP		IMDB		Amazon photos		Amazon computers		MAG	
Algorithm	NMI	ARI	NMI	ARI	NMI	ARI	NMI	ARI	NMI	ARI	NMI	ARI
DMGI	0.703	0.747	0.732	0.790	0.197	0.200	-	-	-	-	OOM	
HDMI	0.695	0.732	0.706	0.761	0.162	0.142	-	-	-	-	OOM	
URAMN	0.717	0.766	0.735	0.798	**0.248**	**0.264**	-	-	-	-	OOM	
O2MAC	0.667	0.716	0.669	0.705	0.135	0.139	-	-	-	-	OOM	
MVGC	0.645	0.641	0.742*	0.804*	0.118	0.126	-	-	-	-	OOM	
MCGC	0.709	0.763	0.716	0.771	0.164	0.186	0.595	0.449	0.557	0.419	OOM	
MvAGC	0.603	0.636	0.650	0.708	0.191	0.201	0.558	0.384	0.512	0.365	0.049	0.004
MAGC	0.597	0.659	0.771	0.827	0.057	0.062	0.591	0.384	0.323	0.158	>12h	
SMGF	**0.718**	**0.768**	**0.776**	**0.830**	0.213	0.224	**0.685**	**0.621**	**0.588**	**0.446**	**0.566**	**0.481**

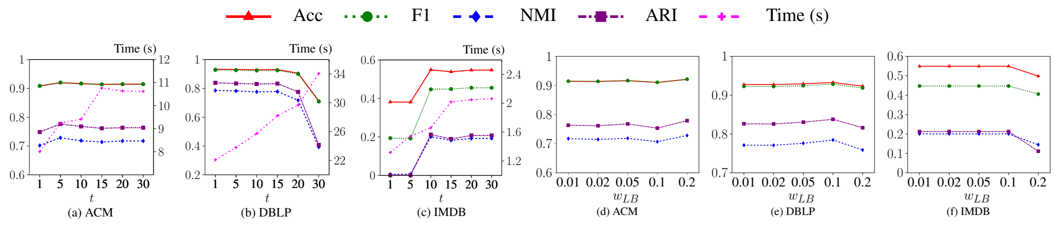

Figure 3: Plots (a)-(c): clustering performance and efficiency with varied parameter t. Plots (d)-(f): clustering performance with varied w_{LB}.

Table 4: Ablation study on ACM, DBLP, and IMDB dataset

	ACM					DBLP						IMDB				
	NMI	ARI	w_1	w_2	w_3	NMI	ARI	w_1	w_2	w_3	w_4	NMI	ARI	w_1	w_2	w_3
UNIFORM	0.611	0.577	0.33	0.33	0.33	0.756	0.815	0.25	0.25	0.25	0.25	0.007	0.002	0.33	0.33	0.33
REG	0.665	0.693	0.20	0.31	0.49	0.777	0.833	0.05	0.36	0.54	0.05	0.016	0.005	0.11	0.28	0.61
GAP-ONLY	0.702	0.748	0.34	0.05	0.61	0.786	0.839	0.02	0.60	0.03	0.35	0.003	0.001	0.39	0.35	0.26
CON-ONLY	0.705	0.753	0.21	0.14	0.65	0.394	0.408	0.05	0.05	0.85	0.05	0.182	0.190	0.13	0.21	0.66
CON-GAP	0.702	0.748	0.34	0.05	0.61	0.781	0.834	0.05	0.67	0.04	0.24	0.004	0.001	0.35	0.42	0.23
SMGF	0.718	0.768	0.22	0.16	0.62	0.776	0.830	0.11	0.50	0.34	0.05	0.213	0.224	0.19	0.26	0.54

datasets. On the million-scale dataset MAG, most baselines are too slow or run out of memory (OOM), while SMGF discovers high-quality clusters in a reasonable time. Our method also exhibits remarkable efficiency and quality on more metrics (refer to expanded results in Appendix B.1).

Hyperparameter analysis. As depicted in Fig. 3, we study the impact of hyperparameters on four clustering metrics. Specifically, we investigate the effects of w_{LB} and t used in our spectral-guided weighting scheme. Fig. 3(b) shows that excessively prioritizing connectivity by setting $t > 20$ has a detrimental impact on DBLP performance. In Fig. 3(c), a deficiency in connectivity also adversely affects clustering quality in the case of IMDB. On the other hand, Fig. 3(d-f) illustrate that SMGF performs consistently well across a range of relatively small values for w_{LB}.

Ablation study. We perform ablations studies on optimization objectives, to demonstrate the effectiveness of two objective functions and the optimization scheme in Section 3.2. Table 4 compares `SMGF` against variants with uniform view weighting (`UNIFORM`), optimizing relative eigen-gap by Fan et al. (2022) (`REG`), `SMGF` without connectivity (`GAP-ONLY`) or eigen-gap optimization (`CON-ONLY`), `SMGF` with reversed optimization steps (`GAP-CON`). Noticeably, `SMGF` has the best overall performance. `CON-ONLY` causes the dense co-term view in DBLP to be predominant in $\mathcal{L}$ and reduces cluster quality. `GAP-ONLY` underweights the attribute view in IMDB but overly emphasizes the incomplete graph views. These findings underscore the significance of balancing both objectives and provide empirical evidence supporting the efficacy of our optimization scheme.

Extended experiments. `SMGF` also exhibits strong performance when applied to multi-view data comprising solely attribute views, as demonstrated in Appendix B.6. Furthermore, we investigate the choice between `Discretize` and `K-means` for clustering in Appendix B.5.

5 Related Work

In the domain of multiple graph views, also known as multiplex graphs, previous research on node embedding includes works by Zhang et al. (2018) and Zhang & Kou (2022). For clustering on multiple attribute views, the research dates back to Bickel & Scheffer (2004), and a comprehensive survey is conducted by Fang et al. (2023). A few graph fusion approaches to multi-view clustering have been proposed. Zhou & Burges (2007) aggregate the random walk Laplacians without weighting. Nie et al. (2017) construct a well-clustered graph as the centroid of single-view graphs. Zong et al. (2018) optimize view weights by assuming the consensus result to be close to every single view. Kang et al. (2020) leverages this assumption for graph fusion based on structural graph learning.

For multiple graphs with attributes, a few graph learning methods have been developed. `O2MAC`, proposed by Fan et al. (2020), learns node embeddings via a graph auto-encoder model with the adoption of reconstruction loss and self-training clustering. Other methods utilize deep graph infomax (Park et al., 2020; Jing et al., 2021) and contrastive learning (Zhang et al., 2022) for multi-view node representation learning. `MVGC` (Xia et al., 2022) improves `O2MAC` by introducing attribute augmentation and a new loss function derived from block diagonal constraints. Liu et al. (2022) extend the graph auto-encoder model by incorporating attention mechanism and contrastive fusion.

Other approaches utilize graph filtering techniques to construct a consensus graph. Pan & Kang (2021) leveraged graph filtering and contrastive learning regularization to learn a consensus graph from smoothed node representations. `MvAGC` (Lin & Kang, 2021) adopts efficient graph filtering and SVD-based spectral clustering leveraging anchor nodes instead of deep learning. `MAGC` (Lin et al., 2023) exploits higher-order proximity for the optimization of consensus graph.

Results from spectral graph theory (Chung, 1997) have been extensively utilized for graph algorithms, including the spectral clustering algorithm (Shi & Malik, 2000; Ng et al., 2001). A few algorithms have leveraged the spectral graph properties for optimization. Lu et al. (2019) show that minimizing the sum of k smallest eigenvalues of the representation matrix improves the block diagonal property for subspace clustering. Afzalan & Jazizadeh (2019) utilizes the eigengap heuristic to determine the number of clusters automatically. Fan et al. (2022) proposes a relative eigengap objective for automating the choice of hyperparameters in affinity graph construction.

6 Conclusion

In this paper, we present `SMGF`, a graph fusion framework that supports unsupervised learning on multi-view graphs with graph views and attribute views. The underlying graph structure among entities is approximated by multi-view Laplacian $\mathcal{L}$, constructed via weighted graph fusion from all views. We formulated two objectives based on eigenvalues of $\mathcal{L}$, motivated by the inherent k classes and graph incompleteness. View weights are determined by a carefully designed two-step optimization scheme. The resulting $\mathcal{L}$ represents a high-quality graph fusion from all views, as evidenced by `SMGF`'s superior embedding and clustering performance.

Looking ahead, we anticipate conducting further investigations into the spectral properties of $\mathcal{L}$ to refine our approach. Additionally, we plan to extend our proposed unsupervised learning framework to accommodate other complex forms of graph data.

REFERENCES

Milad Afzalan and Farrokh Jazizadeh. An automated spectral clustering for multi-scale data. *Neurocomputing*, 347:94–108, 2019.

N Alon and V. D Milman. Λ1, Isoperimetric inequalities for graphs, and superconcentrators. *Journal of Combinatorial Theory, Series B*, 38(1):73–88, 1985. ISSN 0095-8956.

Steffen Bickel and Tobias Scheffer. Multi-view clustering. In *ICDM*, volume 4, pp. 19–26. Citeseer, 2004.

Fan RK Chung. *Spectral Graph Theory*, volume 92. American Mathematical Soc., 1997.

Jicong Fan, Yiheng Tu, Zhao Zhang, Mingbo Zhao, and Haijun Zhang. A Simple Approach to Automated Spectral Clustering. *Advances in Neural Information Processing Systems*, 35:9907–9921, December 2022.

Shaohua Fan, Xiao Wang, Chuan Shi, Emiao Lu, Ken Lin, and Bai Wang. One2Multi Graph Autoencoder for Multi-view Graph Clustering. In *Proceedings of The Web Conference 2020*, WWW '20, pp. 3070–3076. Association for Computing Machinery, 2020.

Uno Fang, Man Li, Jianxin Li, Longxiang Gao, Tao Jia, and Yanchun Zhang. A Comprehensive Survey on Multi-view Clustering. *IEEE Transactions on Knowledge and Data Engineering*, pp. 1–20, 2023.

Haitao Fu, Feng Huang, Xuan Liu, Yang Qiu, and Wen Zhang. MVGCN: Data integration through multi-view graph convolutional network for predicting links in biomedical bipartite networks. *Bioinformatics (Oxford, England)*, 38(2):426–434, September 2021.

Ruiqi Guo, Philip Sun, Erik Lindgren, Quan Geng, David Simcha, Felix Chern, and Sanjiv Kumar. Accelerating large-scale inference with anisotropic vector quantization. In *International Conference on Machine Learning*, 2020.

Dong Huang, Chang-Dong Wang, and Jian-Huang Lai. Fast Multi-view Clustering via Ensembles: Towards Scalability, Superiority, and Simplicity. *IEEE Transactions on Knowledge and Data Engineering*, pp. 1–16, 2023.

Ming Ji, Yizhou Sun, Marina Danilevsky, Jiawei Han, and Jing Gao. Graph Regularized Transductive Classification on Heterogeneous Information Networks. In *Machine Learning and Knowledge Discovery in Databases*, Lecture Notes in Computer Science, pp. 570–586, 2010.

Baoyu Jing, Chanyoung Park, and Hanghang Tong. HDMI: High-order Deep Multiplex Infomax. In *Proceedings of the Web Conference 2021*, WWW '21, pp. 2414–2424. Association for Computing Machinery, 2021.

Zhao Kang, Wangtao Zhou, Zhitong Zhao, Junming Shao, Meng Han, and Zenglin Xu. Large-scale multi-view subspace clustering in linear time. In *AAAI Conference on Artificial Intelligence*, 2019.

Zhao Kang, Guoxin Shi, Shudong Huang, Wenyu Chen, Xiaorong Pu, Joey Tianyi Zhou, and Zenglin Xu. Multi-graph fusion for multi-view spectral clustering. *Knowledge-Based Systems*, 189:105102, February 2020.

James R. Lee, Shayan Oveis Gharan, and Luca Trevisan. Multiway Spectral Partitioning and Higher-Order Cheeger Inequalities. *Journal of the ACM*, 61(6):37:1–37:30, 2014. ISSN 0004-5411.

Yiran Li, Renchi Yang, and Jieming Shi. Efficient and Effective Attributed Hypergraph Clustering via K-Nearest Neighbor Augmentation. *Proceedings of the ACM on Management of Data*, 1(2): 116:1–116:23, 2023.

Zhiping Lin and Zhao Kang. Graph Filter-based Multi-view Attributed Graph Clustering. In *Proceedings of the Thirtieth International Joint Conference on Artificial Intelligence*, pp. 2723–2729. International Joint Conferences on Artificial Intelligence Organization, 2021.

Zhiping Lin, Zhao Kang, Lizong Zhang, and Ling Tian. Multi-View Attributed Graph Clustering. *IEEE Transactions on Knowledge and Data Engineering*, 35(2):1872–1880, 2023. ISSN 1558-2191.

Liang Liu, Zhao Kang, Jiajia Ruan, and Xixu He. Multilayer graph contrastive clustering network. *Information Sciences*, 613:256–267, 2022. ISSN 0020-0255.

Canyi Lu, Jiashi Feng, Zhouchen Lin, Tao Mei, and Shuicheng Yan. Subspace Clustering by Block Diagonal Representation. *IEEE Transactions on Pattern Analysis and Machine Intelligence*, 41 (2):487–501, February 2019.

Andrew Ng, Michael Jordan, and Yair Weiss. On Spectral Clustering: Analysis and an algorithm. In *Advances in Neural Information Processing Systems*, volume 14. MIT Press, 2001.

Feiping Nie, Jing Li, and Xuelong Li. Self-weighted Multiview Clustering with Multiple Graphs. In *IJCAI*, pp. 2564–2570, 2017.

Feiping Nie, Guohao Cai, Jing Li, and Xuelong Li. Auto-weighted multi-view learning for image clustering and semi-supervised classification. *IEEE Transactions on Image Processing*, 27(3): 1501–1511, 2018. doi: 10.1109/TIP.2017.2754939.

ErLin Pan and Zhao Kang. Multi-view Contrastive Graph Clustering. In *Advances in Neural Information Processing Systems*, volume 34, pp. 2148–2159. Curran Associates, Inc., 2021.

Chanyoung Park, Donghyun Kim, Jiawei Han, and Hwanjo Yu. Unsupervised Attributed Multiplex Network Embedding. *Proceedings of the AAAI Conference on Artificial Intelligence*, 34(04): 5371–5378, April 2020.

Bryan Perozzi, Rami Al-Rfou, and Steven Skiena. DeepWalk: Online learning of social representations. In *Proceedings of the 20th ACM SIGKDD International Conference on Knowledge Discovery and Data Mining*, KDD '14, pp. 701–710. Association for Computing Machinery, August 2014.

Michael JD Powell. *A Direct Search Optimization Method That Models the Objective and Constraint Functions by Linear Interpolation*. Springer, 1994.

Jiezhong Qiu, Yuxiao Dong, Hao Ma, Jian Li, Kuansan Wang, and Jie Tang. Network Embedding as Matrix Factorization: Unifying DeepWalk, LINE, PTE, and node2vec. In *Proceedings of the Eleventh ACM International Conference on Web Search and Data Mining*, WSDM '18, pp. 459–467. Association for Computing Machinery, 2018.

Oleksandr Shchur, Maximilian Mumme, Aleksandar Bojchevski, and Stephan Günnemann. Pitfalls of Graph Neural Network Evaluation, June 2019.

Jianbo Shi and J. Malik. Normalized cuts and image segmentation. *IEEE Transactions on Pattern Analysis and Machine Intelligence*, 22(8):888–905, 2000. ISSN 1939-3539.

Arnab Sinha, Zhihong Shen, Yang Song, Hao Ma, Darrin Eide, Bo-June Hsu, and Kuansan Wang. An overview of microsoft academic service (mas) and applications. In *Proceedings of the 24th International Conference on World Wide Web*, pp. 243–246, 2015.

Daniel A. Spielman. Spectral Graph Theory and its Applications. In *48th Annual IEEE Symposium on Foundations of Computer Science (FOCS'07)*, pp. 29–38, 2007.

Mengjing Sun, Pei Zhang, Siwei Wang, Sihang Zhou, Wenxuan Tu, Xinwang Liu, En Zhu, and Changjian Wang. Scalable multi-view subspace clustering with unified anchors. *Proceedings of the 29th ACM International Conference on Multimedia*, 2021.

Zhiqiang Tao, Hongfu Liu, Sheng Li, Zhengming Ding, and Yun Raymond Fu. Marginalized multiview ensemble clustering. *IEEE Transactions on Neural Networks and Learning Systems*, 31: 600–611, 2020.

Ulrike von Luxburg. A tutorial on spectral clustering. *Statistics and Computing*, 17(4):395–416, 2007. ISSN 1573-1375.

Menghan Wang, Yujie Lin, Guli Lin, Keping Yang, and Xiao-ming Wu. M2GRL: A Multi-task Multi-view Graph Representation Learning Framework for Web-scale Recommender Systems. In *Proceedings of the 26th ACM SIGKDD International Conference on Knowledge Discovery & Data Mining*, KDD '20, pp. 2349–2358. Association for Computing Machinery, August 2020.

Siwei Wang, Xinwang Liu, Xinzhong Zhu, Pei Zhang, Yi Zhang, Feng Gao, and En Zhu. Fast parameter-free multi-view subspace clustering with consensus anchor guidance. *IEEE Transactions on Image Processing*, 31:556–568, 2021.

Xiao Wang, Houye Ji, Chuan Shi, Bai Wang, Yanfang Ye, Peng Cui, and Philip S Yu. Heterogeneous Graph Attention Network. In *The World Wide Web Conference*, WWW '19, pp. 2022–2032, May 2019.

Wei Xia, Sen Wang, Ming Yang, Quanxue Gao, Jungong Han, and Xinbo Gao. Multi-view graph embedding clustering network: Joint self-supervision and block diagonal representation. *Neural Networks*, 145:1–9, 2022. ISSN 0893-6080.

Stella X. Yu and Jianbo Shi. Multiclass Spectral Clustering. In *Proceedings of the Ninth IEEE International Conference on Computer Vision - Volume 2*, ICCV '03, pp. 313. IEEE Computer Society, 2003.

Hegui Zhang and Gang Kou. Role-based Multiplex Network Embedding. In *Proceedings of the 39th International Conference on Machine Learning*, pp. 26265–26280. PMLR, 2022.

Hongming Zhang, Liwei Qiu, Lingling Yi, and Yangqiu Song. Scalable multiplex network embedding. In *IJCAI*, volume 18, pp. 3082–3088, 2018.

Rui Zhang, Arthur Zimek, and Peter Schneider-Kamp. Unsupervised representation learning on attributed multiplex network. *Proceedings of the 31st ACM International Conference on Information & Knowledge Management*, 2022.

Dengyong Zhou and Christopher J. C. Burges. Spectral clustering and transductive learning with multiple views. In *Proceedings of the 24th International Conference on Machine Learning*, ICML '07, pp. 1159–1166. Association for Computing Machinery, June 2007.

Linlin Zong, Xianchao Zhang, Xinyue Liu, and Hong Yu. Weighted Multi-View Spectral Clustering Based on Spectral Perturbation. *Proceedings of the AAAI Conference on Artificial Intelligence*, 32(1), 2018. ISSN 2374-3468.

A Experimental details

A.1 Baseline evaluation

- `DMGI` (Park et al., 2020) We tune the consensus regularization hyperparameter α and l2 regularization coefficient β among $\{0.0001, 0.001, 0.01, 0.1\}$ according to their original implementation (`https://github.com/pcy1302/DMGI`). The result with the highest clustering accuracy is reported.
- `URAMN` (Zhang et al., 2022) In accordance with the original hyperparameter specifications at (`https://github.com/RuixZh/URAMN`), we use the authors' settings for the ACM and DBLP datasets. For IMDB, we tune the margin value ϵ_1 and ϵ_2 in $[0.1, 0.9]$, and tune l2 regularization coefficient λ among $\{0.0001, 0.001, 0.01, 0.1\}$. We list node classification and clustering results derived from intuitive integrated embedding $\hat{\mathbf{H}}$, which generally outperforms consensus embedding $\mathbf{Z}$ in the original paper and our experiments.
- `HDMI` (Jing et al., 2021): We evaluate this node embedding model based on their original implementation (`https://github.com/baoyujing/HDMI`), which runs `K-means` on embedding vectors for the unsupervised node clustering task. Using identical model configuration for all datasets, `HDMI` saves model parameters with the lowest loss to produce the final embedding vectors.
- `O2MAC` (Fan et al., 2020): Following instructions in the `O2MAC` paper, we train this model for 1000 iterations on DBLP and IMDB datasets, and 250 iterations on ACM dataset. Model implementation (`https://github.com/googlebaba/WWW2020-O2MAC`) and hyperparameter configurations are the same for all datasets. Evaluation is performed on the trained model with the lowest loss value.
- `MVGC` (Xia et al., 2022): Among the attribute augmentations proposed in this work, we evaluate the `MVGC`-Euler variant due to its consistent lead in reported performance. Hyperparameter settings are identical across all datasets, configured as specified in the `MVGC` paper. Their source code is available at `https://github.com/xdweixia/NN-2022-MVGC` but requires substantial modifications to work on datasets other than ACM. The model is trained for 100 epochs and performs clustering every five epochs. Although we observe ACM clustering accuracy over 96% at certain epochs during its training process, the loss function continues to improve afterward while cluster quality declines. Respecting the unsupervised nature of clustering, we record the clustering results at the minimum of the loss function for eventual evaluation.
- `MCGC` (Pan & Kang, 2021): As specified in `MCGC` paper, we fix $m = 2$ and $s = 0.5$ for graph filtering. In the graph learning process, we tune α parameter in the range $\{0.001, 0.1, 1, 10, 100, 1000\}$ on each dataset for best performance and use the γ parameter settings in the original implementation (`https://github.com/Panern/MCGC`). Finally, we run the training process to reproduce their reported results.
- `MvAGC` (Lin & Kang, 2021): The balance parameter α and the number of anchors m need to be tuned for each dataset. From the settings of m in the authors' implementation (`https://github.com/sckangz/MvAGC`) and our preliminary experiments, we observe that the number of anchors sufficient for good clustering quality is approximately proportional to the number of nodes in the dataset, so we use $\{n/50-20, n/50, n/50+20\}$ as candidates of m. On ACM and DBLP datasets, we use the α candidates in the source code of `MvAGC` and test all combinations of the two hyperparameters. For the other datasets, we first perform a rough search for α over $\{1, 2, 5, 10, 50, 100, 200, 500, 1000\}$ and then narrow it down to a small interval where clustering accuracy is highest. For instance, on Amazon Photos dataset, the highest accuracy found in the first stage occurs at $\alpha = 200$, and we subsequently try $\{120, 150, 180, 200, 220, 250, 300\}$, eventually setting $\alpha = 250$.
- `MAGC` (Lin et al., 2023): The authors of `MAGC` tuned three hyperparameters in their parameter analysis experiments: trade-off parameter α, smoothing parameter γ, and the order of graph filter k. In our experiment, k takes value from $\{1, 2, 3, 4, 5\}$, α varies in the range $\{0.1, 1, 2, 5, 10, 100, 1000\}$ while γ is fixed to -1 as instructed in the `MAGC` paper. On each dataset, we conduct an exhaustive search over all possible hyperparameter combinations by altering configurations in the original implementation (`https://github.com/sckangz/MAGC`) and select the best result based on accuracy value.

Table 5: Clustering performance on ACM, DBLP and IMDB. Mean results on 10 repeats, with standard deviation in brackets. Running time in seconds. Results marked with $*$ are replicated from the original paper. Best in bold and runner-up underlined.

	ACM					DBLP					IMDB				
Algorithm	Acc	F1	NMI	ARI	Time	Acc	F1	NMI	ARI	Time	Acc	F1	NMI	ARI	Time
`DMGI`	0.907 (0.000)	0.906 (0.000)	0.703 (0.000)	0.747 (0.000)	34.10	0.910 (0.000)	0.901 (0.000)	0.732 (0.000)	0.790 (0.000)	395.7	$\underline{0.582}$ (0.000)	$\underline{0.576}$ (0.000)	0.197 (0.000)	0.200 (0.000)	77.35
`HDMI`	0.900 (0.004)	0.899 (0.004)	0.695 (0.006)	0.732 (0.008)	161.2	0.895 (0.005)	0.885 (0.007)	0.706 (0.009)	0.761 (0.010)	537.9	0.541 (0.025)	0.547 (0.026)	0.162 (0.015)	0.142 (0.022)	245.9
`URAMN`	0.915 (0.000)	0.914 (0.000)	$\underline{0.717}$ (0.000)	$\underline{0.766}$ (0.000)	63.32	0.915 (0.000)	0.910 (0.000)	0.735 (0.001)	0.798 (0.001)	159.5	**0.670** (0.001)	**0.667** (0.001)	**0.248** (0.001)	**0.264** (0.001)	129.7
`O2MAC`	0.895 (0.006)	0.897 (0.006)	0.667 (0.011)	0.716 (0.014)	115.0	0.873 (0.013)	0.865 (0.013)	0.669 (0.024)	0.705 (0.027)	684.1	0.547 (0.048)	0.550 (0.047)	0.135 (0.022)	0.139 (0.031)	679.1
`MVGC`	0.789 (0.190)	0.771 (0.217)	0.645 (0.115)	0.641 (0.198)	1631.2	0.923* (0.000)	0.923* (0.000)	0.742* (0.000)	0.804* (0.000)	1934.7	0.514 (0.009)	0.499 (0.011)	0.118 (0.007)	0.126 (0.009)	1542.7
`MCGC`	$\underline{0.915}$ (0.000)	$\underline{0.916}$ (0.000)	0.709 (0.000)	0.763 (0.000)	748.2	0.902 (0.000)	0.895 (0.000)	0.716 (0.001)	0.771 (0.001)	2245.2	0.567 (0.001)	0.545 (0.001)	0.164 (0.002)	0.186 (0.003)	1551.9
`MvAGC`	0.861 (0.011)	0.862 (0.011)	0.603 (0.024)	0.636 (0.025)	**4.334**	0.874 (0.013)	0.866 (0.013)	0.650 (0.020)	0.708 (0.026)	**5.654**	0.552 (0.007)	0.469 (0.044)	0.191 (0.015)	0.201 (0.015)	$\underline{6.399}$
`MAGC`	0.872 (0.000)	0.872 (0.000)	0.597 ((0.000)	0.659 (0.000)	26.10	$\underline{0.928}$ (0.000)	$\underline{0.923}$ (0.000)	$\underline{0.771}$ (0.000)	$\underline{0.827}$ (0.000)	35.98	0.484 (0.001)	0.424 (0.003)	0.057 (0.001)	0.062 (0.001)	33.69
`SMGF`	**0.916** (0.000)	**0.917** (0.000)	**0.718** ((0.000)	**0.768** (0.000)	$\underline{9.080}$	**0.929** (0.000)	**0.924** (0.000)	**0.776** (0.000)	**0.830** (0.000)	$\underline{26.92}$	0.557 (0.000)	0.453 (0.000)	$\underline{0.213}$ (0.000)	$\underline{0.224}$ (0.000)	**3.596**

Table 6: Clustering performance on Amazon photos, Amazon computers and MAG. Mean results on 10 repeats, with standard deviation in brackets. Running time in seconds.

	Amazon photos					Amazon computers					MAG				
Algorithm	Acc	F1	NMI	ARI	Time	Acc	F1	NMI	ARI	Time	Acc	F1	NMI	ARI	Time
`MCGC`	0.674 (0.001)	0.582 (0.001)	0.595 (0.001)	0.449 (0.001)	5102.4	$\underline{0.569}$ (0.001)	**0.531** (0.001)	$\underline{0.557}$ (0.001)	$\underline{0.419}$ (0.001)	17567.5	OOM				
`MvAGC`	0.615 (0.040)	0.568 (0.032)	0.558 (0.029)	0.384 (0.056)	$\underline{14.98}$	0.516 (0.015)	0.426 (0.014)	0.512 (0.011)	0.365 (0.014)	$\underline{60.20}$	$\underline{0.261}$ (0.000)	$\underline{0.044}$ (0.000)	$\underline{0.049}$ (0.000)	$\underline{0.004}$ (0.000)	**4317**
`MAGC`	0.646 (0.000)	0.571 (0.000)	0.591 (0.000)	0.384 (0.000)	172.1	0.447 (0.000)	0.348 (0.000)	0.323 (0.000)	0.158 (0.001)	507.5	>12h				
`SMGF`	**0.787** (0.000)	**0.713** (0.000)	**0.685** (0.000)	**0.621** (0.000)	**7.61**	**0.595** (0.000)	$\underline{0.510}$ (0.000)	**0.588** (0.000)	**0.446** (0.000)	**27.2**	**0.600** (0.000)	**0.335** (0.000)	**0.566** (0.000)	**0.481** (0.000)	$\underline{7602}$

B Expanded Experiment Results

B.1 Clustering performance evaluation

Tables 5 and 6 present the complete evaluation results of clustering experiments. We include supervised metrics accuracy (Acc) and F1 as well as clustering time costs. There's no randomness in `SMGF` algorithm, while some baseline algorithms show substantial standard deviations in their results.

B.2 Hyperparameter analysis

B.2.1 Varying w_{LB}, the lower bound of view weights

Parameter w_{LB} specifies the lower bound of view weights to ensure that every graph or attribute view of the input multi-view graph contributes to the final clustering results. Our method `SMGF` sets $w_{LB} = 0.05$ by default. Here we test w_{LB} in $\{0.01, 0.02, 0.05, 0.1, 0.2\}$ and present the results in Fig. 4. Observe that the performance of `SMGF` remains table from 0.01 to 0.1 on all datasets; the performance increases at 0.2 on ACM and Amazon Photos but decreases on DBLP and IMDB. Therefore, we set $w_{LB} = 0.05$ by default.

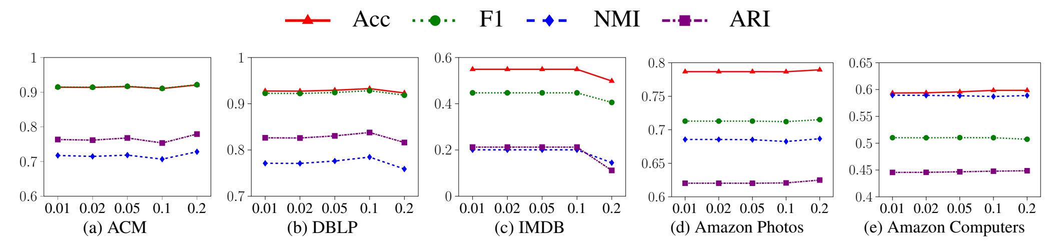

Figure 4: Varying w_{LB}.

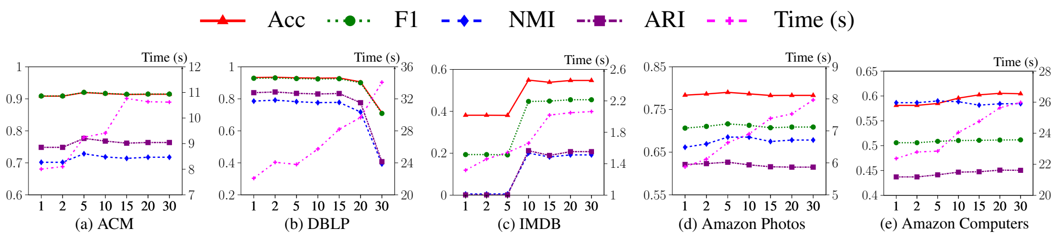

Figure 5: Varying t.

Table 7: Ablation study on ACM, DBLP, and IMDB dataset

	ACM							DBLP								IMDB						
	Acc	F1	NMI	ARI	w_1	w_2	w_3	Acc	F1	NMI	ARI	w_1	w_2	w_3	w_4	Acc	F1	NMI	ARI	w_1	w_2	w_3
`UNIFORM`	0.816	0.815	0.611	0.577	0.33	0.33	0.33	0.923	0.918	0.756	0.815	0.25	0.25	0.25	0.25	0.382	0.195	0.007	0.002	0.33	0.33	0.33
`REG`	0.884	0.886	0.665	0.693	0.20	0.31	0.49	0.930	0.926	0.777	0.833	0.05	0.36	0.54	0.05	0.389	0.215	0.016	0.005	0.11	0.28	0.61
`GAP-ONLY`	0.908	0.909	0.702	0.748	0.34	0.05	0.61	0.933	0.929	0.786	0.839	0.02	0.60	0.03	0.35	0.380	0.190	0.003	0.001	0.39	0.35	0.26
`CON-ONLY`	0.910	0.910	0.705	0.753	0.21	0.14	0.65	0.714	0.709	0.394	0.408	0.05	0.05	0.85	0.05	0.538	0.448	0.182	0.190	0.13	0.21	0.66
`CON-GAP`	0.908	0.908	0.702	0.748	0.34	0.05	0.61	0.931	0.926	0.781	0.834	0.05	0.67	0.04	0.24	0.381	0.192	0.004	0.001	0.35	0.42	0.23
`SMGF`	0.916	0.917	0.718	0.768	0.22	0.16	0.62	0.929	0.924	0.776	0.830	0.11	0.50	0.34	0.05	0.557	0.453	0.213	0.224	0.19	0.26	0.54

Table 8: Ablation study on Amazon Photos & Computers dataset

	Amazon photos							Amazon Computers						
	Acc	F1	NMI	ARI	w_1	w_2	w_3	Acc	F1	NMI	ARI	w_1	w_2	w_3
`UNIFORM`	0.789	0.717	0.686	0.623	0.33	0.33	0.33	0.605	0.515	0.578	0.427	0.33	0.33	0.33
`REG`	0.777	0.698	0.653	0.610	0.18	0.63	0.19	0.602	0.512	0.585	0.449	0.42	0.53	0.05
`GAP-ONLY`	0.784	0.706	0.661	0.621	0.18	0.31	0.51	0.582	0.505	0.587	0.437	0.52	0.05	0.43
`CON-ONLY`	0.783	0.708	0.676	0.616	0.33	0.62	0.05	0.607	0.512	0.584	0.452	0.39	0.56	0.05
`CON-GAP`	0.779	0.700	0.655	0.613	0.18	0.58	0.24	0.581	0.506	0.586	0.437	0.55	0.05	0.40
`SMGF`	0.787	0.713	0.685	0.621	0.36	0.56	0.08	0.595	0.510	0.588	0.446	0.47	0.43	0.10

B.2.2 VARYING CONNECTIVITY REGULARIZATION ITERATIONS t

Parameter t is the number of optimization iterations during which we maximize the connectivity objective function f_{CON}. `SMGF` sets $t = 10$ by default. To assess the impact of regularization on performance, we experiment with various settings of t in $\{1, 2, 5, 10, 15, 20, 30\}$. As shown in Fig. 5, the first 10 iterations of connectivity regularization improve cluster quality on all datasets except DBLP. When t reaches 20, we notice a decline in DBLP clustering quality caused by the excessive weight assigned to the highly dense Co-Term graph view. Larger t also leads to a longer execution time. We conclude that setting $t \in [10, 20]$ generally yields favorable performance, and $t = 10$ is a reasonable choice for better efficiency.

B.3 ABLATION STUDY

We perform ablation studies on `SMGF`, with expanded results in Tables 7 and 8. `UNIFORM` is a vanilla version where weights are uniformly assigned to the z views without further optimization. Three alternative methods where `COBYLA` optimizes a single objective till convergence are also tested, including `REG` (relative eigengap) (Fan et al., 2022), `GAP-ONLY` (eigengap objective only,

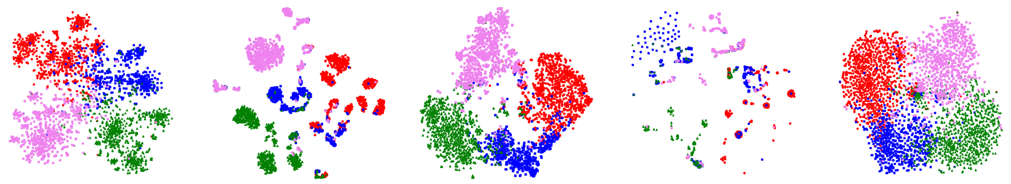

(a) SMGF (b) HDMI (c) DMGI (d) O2MAC (e) URAMN

Figure 6: Visualization of node embeddings obtained from DBLP dataset.

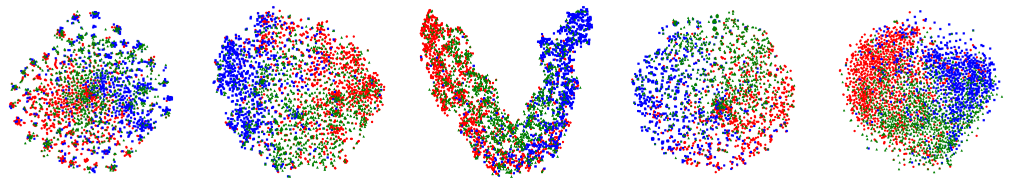

(a) SMGF (b) HDMI (c) DMGI (d) O2MAC (e) URAMN

Figure 7: Visualization of node embeddings obtained from IMDB dataset.

Eq. 3) and CON-ONLY (connectivity objective only, Eq. 4). The maximization objective of relative eigengap is formulated as $f_{reg}(\mathcal{L}) = (\lambda_{k+1}(\mathcal{L}) - \frac{1}{k}\sum_{i=1}^{k}\lambda_i(\mathcal{L}))/(\frac{1}{k}\sum_{i=1}^{k}\lambda_i(\mathcal{L}) + \epsilon)$, where $\epsilon = 10^{-5}$. Results of the ablation study on five datasets are reported in Tables 7 and 8. In these tables, in addition to Acc, F1, NMI, ARI, and time, the weights of all views in a dataset are also reported. As shown in these tables, on all five datasets, SMGF exhibits superior consistency in performance, which validates the effectiveness of the proposed eigengap and connectivity objectives in Sections 3.2.1 and 3.2.2. Furthermore, as shown in results on DBLP dataset (see Table 7), CON-ONLY without eigengap objective assigns a rather large weight 0.85 to w_3; however, the corresponding graph view is quite dense with highly connected nodes. When only the connectivity objective is considered, this view dominates the clustering process with excessive weight. On the other hand, SMGF, with the consideration of both eigengap and connectivity objectives, addresses this issue with a more suitable weight assignment, which demonstrates the effectiveness of the two-stage optimization scheme described in Section 3.2.3.

B.4 Visualization of embedding vectors

For DBLP and IMDB datasets, Fig. 6 and Fig. 7 present the t-SNE visualization of embedding vectors acquired by SMGF and four baseline approaches.

B.5 Discretize vs K-means

Spectral clustering is a two-phased algorithm where we first perform eigendecomposition and then calculate discrete labels from eigenvectors. For the second step, SMGF adopts the method proposed by Yu & Shi (2003), referred to as Discretize. K-means is another common alternative in preceding works, and we experimentally evaluate their effectiveness. From the results presented in Table 9, we observe that using Discretize and K-means leads to similarly competitive performance. Nevertheless, K-means occasionally exhibits instability in clustering quality and is consistently less efficient than Discretize.

B.6 Mutli-view attribute clustering

Note that it is not our focus in this paper to handle multi-view data consisting of purely attribute views. Nevertheless, it is indeed possible to adapt SMGF for general multi-view data without any

Table 9: Clustering performance of `K-means` and `SMGF` on five datasets. Mean results on 10 repeats, with standard deviation in brackets. Running time in seconds. Best in bold.

	ACM					DBLP					IMDB				
Algorithm	Acc	F1	NMI	ARI	Time	Acc	F1	NMI	ARI	Time	Acc	F1	NMI	ARI	Time
`K-means`	0.912 (0.000)	0.912 (0.000)	0.714 (0.001)	0.756 (0.001)	14.189	0.928 (0.000)	**0.924** (0.000)	**0.776** (0.000)	0.827 (0.000)	35.02	0.541 (0.000)	0.444 (0.000)	0.194 (0.000)	0.195 (0.000)	**2.489**
`SMGF`	**0.916** (0.000)	**0.917** (0.000)	**0.718** ((0.000)	**0.768** (0.000)	**9.080**	**0.929** (0.000)	**0.924** (0.000)	**0.776** (0.000)	**0.830** (0.000)	**26.92**	**0.557** (0.000)	**0.453** (0.000)	**0.213** (0.000)	**0.224** (0.000)	3.596

	Amazon photos					Amazon computers				
Algorithm	Acc	F1	NMI	ARI	Time	Acc	F1	NMI	ARI	Time
`K-means`	0.751 (0.003)	0.664 (0.002)	0.633 (0.003)	0.531 (0.009)	9.683	**0.597** (0.047)	**0.530** (0.005)	0.551 (0.002)	0.359 (0.036)	36.82
`SMGF`	**0.787** (0.000)	**0.713** (0.000)	**0.685** (0.000)	**0.621** (0.000)	**7.61**	0.595 (0.000)	0.510 (0.000)	**0.588** (0.000)	**0.446** (0.000)	**27.2**

Table 10: Multi-view attribute datasets

Name	n	Attributes (d_X)	k
Yale	165	Intensity (4,096), LBP (3,304), Gabor (6,750)	15
ALOR	10,800	Similarity (77), Haralick (13), HSV (64), RGB (125)	100
NUS-WIDE	30,000	CH (64), CM (225), CORR (144), EDH (73), WT(128)	31

Table 11: Clustering performance for multi-view attribute data.

	Yale			ALOI			NUS-WIDE		
Algorithm	ACC	F1	NMI	ACC	F1	NMI	ACC	F1	NMI
`SwMC`(Nie et al., 2017)	0.612	0.663	0.448		OOM			OOM	
$\mathtt{M^2VEC_{km}}$(Tao et al., 2020)	0.452	0.485	0.204		OOM			OOM	
$\mathtt{M^2VEC_{spec}}$(Tao et al., 2020)	0.440	0.501	0.236		OOM			OOM	
`LMVSC`(Kang et al., 2019)	0.552	0.616	0.373	0.566	0.750	0.450	0.121	0.086	0.024
`SMVSC`(Sun et al., 2021)	0.570	0.617	0.376	0.343	0.574	0.170	0.178	0.114	0.053
`FPMVS-CAG`(Wang et al., 2021)	0.442	0.498	0.253 7	0.315	0.555	0.161	**0.194**	0.123	**0.064**
`FastMICE`Huang et al. (2023)	**0.642**	0.679	0.467	0.756	0.834	0.664	0.144	0.134	0.051
`SMGF`	0.636	**0.683**	**0.492**	**0.808**	**0.855**	**0.689**	0.151	**0.152**	0.059

predefined graph structure. Specifically, `SMGF` handles such data by transforming each attribute view to the normalized Laplacian of its KNN graph.

We perform additional experiments on 3 datasets: Yale, ALOI, and NUS-WIDE, with statistics and experimental results provided in Table 10 and 11. It is remarkable to observe that our `SMGF` is powerful enough to achieve comparable or outstanding performance on these multi-view datasets, compared with existing methods. The evaluation results of baseline algorithms are transcribed from Huang et al. (2023).

B.7 Visualization of optimization process

In this section, we closely examine the optimization process of eigen-gap and connectivity objectives in `SMGF`. Specifically, the goal is to find out whether the first optimization step maximizes the eigen-gap and how much it deteriorates when connectivity is maximized in the next step.

To demonstrate the distribution of two objectives over the constrained space of weight parameters, we sample view weight combinations via an exhaustive grid search at an interval of 0.05. The corresponding objective values are plotted as the x/y coordinates of dots in Fig. 8. As the eigen-gap is optimized (Stage 1), the red line is the locus of objectives corresponding to the weight parameters updated in each iteration. On every dataset, we observe that view weights converge towards a local

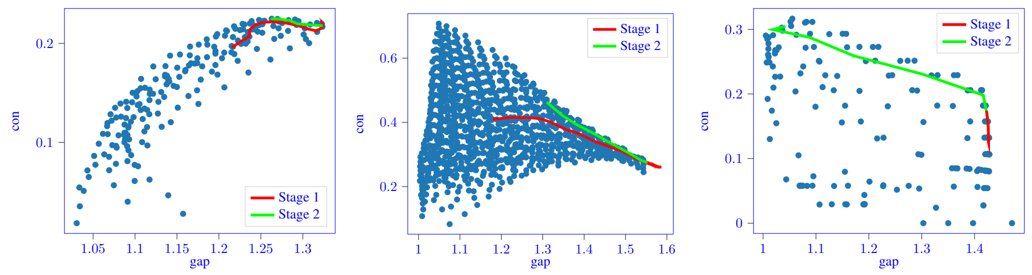

(a) ACM (b) DBLP (c) IMDB

Figure 8: Visualization of the optimization process of eigen-gap and connectivity objectives.

optimum of eigengap (on IMDB, the trajectory is directed downwards). This implies a positive answer to our first question and suggests a continued manifold exists for the eigengap.

The green line that starts from the endpoint of Stage 1 illustrates the trajectory of connectivity optimization. On every dataset, this locus moves towards the top-left direction, which indicates a trade-off between two objectives. We also notice that the green line extends along the boundary of dots, which suggests that the update of view weights approximately traverses the Pareto front of the eigengap and connectivity objectives. In other words, the eigengap is maintained as large as possible while improving connectivity. These results validate that `SMGF` optimizes both objectives and balances them.